TIME SERIES ANALYSIS OF NOAA-AVHRR IMAGES OF LAKE NAIVASHA BASIN (KENYA)

A.H. Fathy[1] , A.S. M. Gieske[2] and A.M.J. Meijerink[3]

[1]Ministry of Public Works and Water Resources, Cairo, Egypt
[2] International Institute for Aerospace Survey and Earth Sciences, P.O. Box 6, 7500 AA Enschede, The Netherlands, gieske@itc.nl
[3] International Institute for Aerospace Survey and Earth Sciences, P.O. Box 6, 7500 AA Enschede, The Netherlands, meijerink@itc.nl

KEYWORDS: NOAA-14 composite images, level 1B, time series analysis, NDVI, evaporation, cloud correction, radiometric correction, noise filtering.

ABSTRACT

Study of hydrological behavior of large-scale catchments is a crucial step in all aspects of water resources management. Remote sensing imagery is one of the increasingly important tools in acquiring spatial and temporal information on such catchments. In this paper a time series of public domain NOAA-AVHRR ten-day composite images was used to study an area in Lake Naivasha Basin (Kenya). Several different techniques of time series analysis were employed, linking the existing ILWIS 2.2 GIS/RS software to a number of subroutines in C, handling, for example, Fourier analysis, noise filtering and cloud correction algorithms.

Lake Naivasha Basin was divided into a number of primary hydrological zones (terrain mapping units) on the basis of previous work in the area. The hydrological behaviour of the hydrological response variables, such as NDVI and evaporation, was derived from NOAA/AVHRR channels 1, 2, 4 and 5, combined with ancillary data on elevation and rainfall in the different terrain units.

The assessment of the hydrological behaviour of the different terrain units has shown that some of these share the same characteristics and can therefore be combined into a single hydrological unit. Furthermore, the statistical techniques used to reduce the noise-to-signal ratio in the vegetation profile proved to be a successful alternative for radiometric correction techniques, which require detailed information on the underlying interactions between the signal and the atmosphere. It is recommended that further work be done with respect to the ecological characteristics that affect the hydrological behavior of the different zones in the basin. Information on soil, geology, land cover and topography can be combined with hydrological response variables derived from this type of analysis. It is also recommended that the work is extended using the raw level 1B data available from the Satellite Active Archive.

1. INTRODUCTION

Optimization of the usage of the available water resources in a large-scale catchment is a crucial issue, because of the limited amount of water against the demand by increase of population. To achieve this optimization, a thorough understanding of the hydrological behavior of the catchment is required in the sense that this is the first step in the management process of the water resources. One way to acquire a better understanding is to use remote sensing data. By using derived hydrological response variables, such as, for example, vegetation indices, surface temperature, and surface albedo from remote sensing imagery, and the relation between these response variables and the different components of the hydrological cycle, an assessment of the catchment's hydrological behavior can be made. Different sources of noise exist in satellite images which may affect the image interpretation. Before starting the analysis phase of any study this noise should be removed to a degree depending on the accuracy required and the purpose of the analysis. Noise sources include atmosphere, soil background, inaccurate geo-referencing and image resolution. In this study the possibility was investigated of making use of a series of NOAA-AVHRR composite satellite images downloaded from the Internet (Eidenshink and Faundeen, 1994), to study the hydrological behavior of the study area. An area in Kenya around Lake Naivasha was selected as study area (see Fig. 1). The series of images was processed using the existing techniques of image processing available in ILWIS2.2 software, linked to subroutines written in C and developed for the purpose of handling Fourier analysis, noise filtering and cloud correction. The main objectives of this study are

- to establish a methodology to process a time series of satellite images data to derive reliable hydrological response variables
- and to create an interface between GIS and time series analysis techniques to arrive at an assessment of a catchment's hydrological behavior.

August 16-20. 2nd ORS 1999 ITC

2. METHODOLOGY

The NOAA-AVHRR composite images used in this study are data downloaded from the Internet Web Site "http://edcwww.cr.usgs.gov/landdaac", (Eidenshink and Faundeen, 1994), and the Digital Elevation of the World at resolution of 30 arc seconds.

NOAA-AVHRR series

Currently, NOAA-AVHRR composite images are available from April 1992 to January 1996. There is a data gap period during the time that NOAA-11's orbit decayed to the point that the local overpass times were so late in the afternoon that severe sun angles were encountered which made the data scientifically questionable. The data gap starts in October 1994 and ends in January 1995. The rest of the data starting from February 1995 till January 1996 were recorded using NOAA-14 satellite. The data set is made up of 5 channels raw AVHRR data, at 1.1-km resolution (at nadir) from each daily afternoon pass over all land and coastal zones using data from NOAA's polar-orbiting TIROS. The available channels and bands in each 10-day record are in Table 1.

band	description
1	AVHRR channel 1
2	AVHRR channel 2
3	AVHRR channel 3
4	AVHRR channel 4
5	AVHRR channel 5
6	NDVI
7	Satellite Zenith Angle
8	Solar Zenith Angle
9	Relative Azimuth
10	Date Index

Table 1. Available channels in the data set.

The image data base

The database of images, which were used to derive the response variables consists of the following downloaded images:

1. the visible channel (channel 1)
2. the near infrared channel (channel 2)
3. the brightness temperature (channel 4)
4. the brightness temperature (channel 5)

To construct a continuous time series of images, the gap existing for October, November, December 1993, the entire year of 1994 and January 1995 has to be covered. Decadal NDVI images for these months were created for these months using the maximum value from the same decade and the same month available from the pervious and next year. Images for channels 1, 2, 4, and 5 were created by assigning the corresponding value of the maximum NDVI for the same channel to the pixels in the images. Finally, shifting the 1995 images back to 1994 covered the 1994-year gap and allowed construction of a continuous series of 32 months.

Pre-Processing

The pre-processing (Eidenshink and Faundeen, 1994) consisted of the following steps:

- Georeferencing, including elevation corrections
- Resampling of the images to 1 km pixel size
- Radiometric and atmospheric corrections computation of composite images for 10 day periods, leading to 10 day maximum NDVI values.

Digital Elevation Model (DEM)

The Digital Elevation Model (DEM) of the study area has been derived from the public domain GTOPO30 global digital elevation model (DEM). The characteristics of the data set and a description of the processing steps of the input file are as follows:

- Elevations in GTOPO30 are regularly spaced at 30-arc seconds (approximately 1 kilometer).
- The DEM is provided as 16-bit signed integer data in a simple binary raster.
- Data sources for Africa have been derived from the Digital Terrain Elevation Data and the Digital Chart of the World
- The accuracy for these data sources are expected to be + or - 30 meters at 90 percent confidence for the Digital Terrain Elevation Data, and for + or - 160 meters for the Digital Chart of the World.

Through a C subroutine the binary elevation file was converted to ILWIS 2.2 raster format, which was then georeferenced to the same coordinate system as the other data sources.

Image Classification

As has been mentioned above, the criteria and the accuracy of the classification used to divide the study area into classes, is of great importance in the interpretation of the results. In this study the classification criteria were based on dividing the study area into Terrain Mapping Units in which each unit has its own landform with different attributes of geology, soil, and land cover (Fig. 2). This map was based on previous work in the area (Hamududu, 1998).

Derivation of response variables

The response variables, the Normalized Difference Vegetation Index (NDVI), the Soil Adjusted Vegetation Index (SAVI), surface reflectance (albedo), and Surface Temperature, were derived from the available downloaded channels of NOAA-AVHRR data by using the map calculation functions of ILWIS2.2 software and the C-subroutines. Map lists for the time series of images were prepared for further processing with the C-program.

3. FURTHER GEOMETRIC, RADIOMETRIC AND CLOUD CORRECTIONS

Geometric corrections

As has been mentioned before in the processing flow part, the images in the data set were geometrically registered. However, to combine the data set images with data sets from other sources, the images had to be georeferenced again. In recognizing ground control points with images of low resolution, as is the case of NOAA images, it proved only possible to use lakes in the study area like Lake Naivasha and Lake Nakuru as ground control features. The master image for image to image geoeferencing was a TM image available in the ITC. It was estimated that the error is in the order of one or two pixels.

Cloud Contamination

To use NOAA-AVHRR images in extracting information about the land surface characteristics and to make estimates of surface variables such as land surface temperature and vegetation indices, cloud free pixels have to be identified. For the study area in Kenya there are two rainy seasons and hence the chance of having cloud contaminated pixels is high, which constitutes a severe problem in studying the time series of surface variables through remote sensing.

The technique that is used in this study, is the "threshold technique" developed by Saunders and Kriebel (1988). The gross cloud test, which uses channel 5 brightness temperature, and the near-infra red reflectance (channel 2) to visible reflectance (channel 1) ratio test have been used.

Gross cloud test

Because the study area is a mountainous area special care has to be taken when selecting the threshold, because the decrease in air temperature with altitude must be taken into account to avoid misclassifying cold cloud-free pixels as cloud contaminated. A non-constant threshold has been adopted in this study. The variable threshold was determined using the DEM map and the relation between altitude and mean maximum temperature for the different months of the year.

The mean maximum temperature has been adopted since the satellite passes over the study area at 2:30 pm and at this time the air temperature is supposed to be at maximum. The threshold was determined by subtracting a value of 6 degrees from the air temperature as determined from the altitude-temperature relationship.

A map list for the time series of channel 5 brightness temperature images for the catchment area has been prepared using ILWIS 2.2 for the cloud detection process function, including the entire time series.

The NIR/VIS ratio test

A map list of the time series of the ratio images has been prepared and wasused as input for the cloud detection function together with the map list of channel 5 brightness temperature.

Every pixel in the response variable images is checked for cloud contamination, and the pixel, which does not satisfy the conditions of the two tests i.e. pixels whose brightness temperature below the brightness temperature threshold or whose NIR/VIS ratio below the ratio threshold is flagged as cloud contaminated.

The performance of the cloud detection algorithm

An image has been generated by applying the cloud detection and the spatial filter algorithm for the NDVI image of the last decade in January 93. Figs 3 and 4 show the NDVI image respectively before and after application of the cloud correction algorithm. Comparison of these two images shows that cloud contaminated pixels in the upper right corner (i.e. the highest part of the study area) have been removed to a large extent.

The Mean and Standard Deviation screening

To remove the redundant noise caused by the atmosphere and the haze, another screening algorithm was applied for the Surface Temperature, Vegetation Index and Surface Albedo for every class in the study area. The different steps of the algorithm have been implemented with a C-subroutine according to the following procedure suggested by Gutman (1991)

- The input for the function is the supposedly cloud-free pixels for every class.
- The average and the standard deviation of the remaining pixels are calculated.
- Every pixel in the class is restricted to vary within the standard deviation of the means of the different response variables. The threshold is as follows:

$$| \langle X \rangle - X | < \text{std}(X) \qquad (1)$$

where:

<X>is the mean for every class
X is the value of the pixel
std(X) is the standard deviation of the class.

- The average of the Pixels that passes the threshold test is calculated for every class for the above mentioned response variables.
- The output of the function is the input for the smoothing function of the Vegetation Index response variable.

Atmospheric correction

One of the most complex factors affecting signal reception, is the atmosphere. This complexity stems from the high spatial and temporal variability of constituents of the atmosphere,

which cause attenuation of the signal and consequently affect the signal-to-noise ratio. Most of the approaches suggested to address variable atmospheric attenuation of surface observations require either knowledge of the meteorological variability of the atmosphere parameters, or knowledge of the observed surface reflectance (Goward et al., 1991). Since there no data were available for the temporal and spatial distribution of aerosols and water vapor within the framework of this study and because water bodies have been masked in this data set, other techniques for radiometric corrections were employed in this study. Van Dijk et al. (1987) has devised the method that was used in this study. This method reduces the noise-to-signal ratio found in remotely sensed data without precise knowledge of the underlying interactions, using standard methods of time series analysis. The noise N(t) is known to consist of very high frequency components compared to the signal S(t). Smoothing is an attempt to reduce the amount of noise and make the signal the main component of the curve. For example, in studying vegetation index profiles, the vegetation index, which reflects the green-up of vegetation during the growing season has frequency waves of several weeks. This can be regarded as the signal component of the profile The radiometric disturbance caused by atmospheric attenuation and viewing angles and other sources is changing frequently and consequently adds a high frequency component or noise to the signal. Two techniques for filtering have been used in this study: i.e. compound smoothing. (Velleman and Hoaglin, 1981) and Fourier filtering. The procedure requires the use of the terrain mapping units map and the map list for the time series of NDVI images.

4. HYDROLOGICAL RESPONSE VARIABLES

NDVI/SAVI

Through the filtering and smoothing methods described in the previous section a map list of NDVI/SAVI variables was prepared.

Surface temperature

The split window technique is used in this study to derive surface temperature. This technique uses channels 4, 5 in NOAA AVHRR series. Two techniques have been used for comparison and to help choosing the most suitable one for the study area. Both were developed by Caselles et al. (1994). They also developed the quadratic split-window algorithm. This nonlinear algorithm takes into account the atmospheric variability on a global scale (Eqns 2 and 3). Parameters α and β were derived for the HAPEX-Sahel area (13-14N; 2-3E), in which it was suggested to use α equal to 40 K and β equal to 30 K. These values have been adopted in the present study.

$$T=T_4+[a_0+a_1 (T_4 - T_5)](T_4 - T_5) + B(\varepsilon) \quad (2)$$

where:

T is the surface temperature
T_4 is the channel 4 brightness temperature
T_5 is the channel 5 brightness temperature
a_0 , a_1 are coefficients of the regression

$B(\varepsilon)$ is the emissivity dependent parameter.

$$B(\varepsilon) = \alpha(1- \varepsilon_4) - \beta\Delta\varepsilon \quad (3)$$

CASE	A_o	A_1	α	β
Midlatitude Winter	1	0.58	50	150
Midlatitude Summer	1	0.58	50	75
Tropical	1	0.58	40	30

Table 2, coefficients for the quadratic split window equation

Emissivity values have been calculated based on the following equation (Van de Griend et al., 1993), applicable to semi-arid areas:

$$\varepsilon= a + b * \ln(NDVI) \quad (4)$$

where a = 1.0094 and b= 0.047. An assumption has been made for the value of emissivity in band 4 (ε_4) that it is equal to broad band emissivity and the difference in emissivity between channel 4 and 5 is equal to -0.004.

The second equation is a linear one derived from work in Spain (equation 5). The equation was used here because of the similarity in environment between the study area and the area in which the equation has been tested

$$T=T_4+2.13(T_4-T_5)+.18+50(1- \varepsilon_4)-200\Delta\varepsilon \quad (5)$$

where:

T is the surface temperature
T_4 is the channel 4 brightness temperature
T_5 is the channel 5 brightness temperature
ε_4 is the emissivity in band 4
$\Delta\varepsilon$ is the difference in emissivity between channels 4 and 5

Therefore values of the surface temperature for the different classes on a decadal basis during the study period have been calculated based on the mean value of NDVI, as well as on channel 4 and channel 5 brightness temperatures. Since there are numerous equations for the split window technique, the correlation between the two selected equations for the different classes was checked to verify the use of one of them and the accuracy of the surface temperature estimation. Three Terrain Mapping Units were selected to represent the catchment. The first one is the mountainous area with forest land cover, the second is the Lava with natural vegetation and bare rocks land cover, and the third one is the volcanic plateau with rain-fed agriculture and grass land cover. The results indicate a high correlation between the two methods in the three units. Therefore surface temperature from the global equation was used in this study.

Surface Albedo

One of the approaches in albedo analysis has been described in the NOAA Technical Report NESDIS 49 (1990). The equation used is as follows:

$$BB = 0.7459 + 0.347\ A_1 + 0.65\ A_2 \quad (6)$$

where:

BB is the broadband albedo (%)
A_1 is the reflectance of channel 1 (%)
A_2 is the surface reflectance of channel 2 (%).

5. CATCHMENT ZONATION

In this part the temporal and spatial consistency of the output results of the individual response variables for the different Terrain Mapping Units (TMU's) is discussed first. Secondly, a pair-wise consistency is applied by studying the interrelationship between the response variables spatially and temporally. Thirdly, the hydrological behavior of the different TMU's is qualitatively assessed. Hydrological zonation of the catchment is mainly based on the analysis of the time series of a surface temperature-NDVI. Fourier analysis was used to analyze the NDVI time series, since this is a periodic function in time. The analysis of surface temperature and albedo was based on the differences in TMU values because they exhibit high frequency behavior due to their immediate response to rainfall

The Normalized Difference Vegetation Index (NDVI)

The dynamic behavior of vegetation for the different classes was studied through Fourier analysis. Both amplitude and phase of the main components were used to analyze the dynamic behavior of the vegetation. It was noticed for almost all the TMU's that six and seven-month components have been detected. This might be explained by the short period of the time series, which could be affected by climatic changes from one year to another, for example the onset of the rainy season. The six- and seven-month components were combined into one component ("A" component). The amplitude and onset for the main components were plotted for the different Terrain Mapping Units (Fig. 5). It can be concluded that most of the Terrain Mapping Units land covers in the catchment follow a bimodal rainfall pattern, which characterizes the catchment area. The existence of a four-month component in some classes seems reasonable based on fieldwork information, but some detected components cannot be explained. A dominant one-year component is observed in the forest area and in the bare rock and natural vegetation area. Phase also seems to be reasonable since most of the land covers reaches its highest value almost by the end of the rainy season.

Surface Temperature

It was mentioned before that two satellites, NOAA 11 and NOAA 14 have recorded the data set. It has been found that there is a difference between channel 4 and 5 values in the two data sets. Values recorded by NOAA 14 tend to give higher values than values recorded by NOAA 11. This may be explained by the different calibration coefficients or by the difference in the time of the satellite overpass. The spatial consistency is tested with respect to the land cover of the Terrain Mapping Unit (TMU).

Surface Reflectance (Albedo)

Surface reflectance is an instantaneous value that is affected by many factors like, among others, surface wetness, canopy structure and land cover. Therefore, surface albedo depends also on the season and on the phase of vegetation growth. The consistency of the calculated surface albedo is tested based on the spatial and temporal pattern, as was done for surface temperature. The average annual value for surface albedo for the different classes ranges between 17% to 20%. The lowest value was for forest area (17%) which appears reasonable compared to values in literature. The average value for the Lava TMU was found to be the lowest, which appears to be correct since this area is located in high areas receiving more frequent and higher annual rainfall. In this area the fraction of exposed soil is high so when it rains the soil becomes wet and consequently surface albedo becomes less. Average values of surface albedo for rainy and dry seasons are shown in Fig. 6. From the graph we can see that the average value for the rainy season is lower than the dry season for all the classes. This seems reasonable since rainfall is one of the factors that affects the surface reflectance.

NDVI-surface temperature relationship

Investigating the relationship between NDVI and surface temperature is difficult, because surface temperature measurement are instantaneous. Some changes in temperature occur rapidly, for example, after heavy rain. On the other hand NDVI measurements are related to the vegetation's behaviour which changes more slowly. This means that there is a time lag between the vegetation and surface temperature response to rainfall. In warm regions of Africa as in the study area, changes in Vegetation Indices like NDVI are expected to be negatively correlated to surface temperature (Lambin and Ehrlich, 1996). The monthly maximum NDVI values have been studied as a function of the monthly maximum surface temperature for one year starting from October 1992 until September 1993 for the whole catchment to avoid the effect of instantaneous events as much as possible. It was found that there is a negative relationship between NDVI and surface temperature. The correlation between the two variables varied between the different months.

Surface Temperature Albedo relationship

The relationship was found to be positive until a certain albedo threshold value and then turns to be negative. Bastiaanssen (1995) proved that relationship pattern in Egypt by taking

measurements in a transect from wet to dry areas. In this research since the data set is ten days composite, pixel values were not necessarily extracted from the same day. Therefore the relationship was tested by taking a transect through all the classes in one decade in the dry season and in another one in the rainy season. Fig. 7 illustrates this relationship despite the scatter in points.

The output can be used in two ways. Firstly to drive a qualitative assessment of the evapotranspiration of the different units in the study area, which, in turn, leads to a qualitative assessment of the hydrological behaviour of these units and consequently for the study area as a whole. Secondly, further work can be done on quantification of evapotranspiration using the Surface Energy Balance Algorithm for Land (SEBAL) (Bastiaanssen, 1995)

Hydrological Zonation of the Catchment

The time series for the arctangent of the ratio between surface temperature and vegetation index (NDVI), was used to study the hydrological behavior of the different Terrain Mapping Units (TMU's) and to try and make a hydrological zonation of the study area. The average values of the arctang(Ts/NDVI) and the six-month amplitude values for the different Terrain Mapping Units were plotted in the feature space to illustrate the distinction between these classes. Fig. 8 illustrates the feature space between phase and amplitude.

6. CONCLUSIONS

In this study a methodology was established to process a time series of images together with ancillary data. The processing has been implemented through integration between GIS software "ILWIS 2.2" and C-subroutines. The program processes the time series of images and the ancillary maps in an automated way and creates an interface between the GIS software, and methods for noise removal and Fast Fourier Transformation functions to decompose the time series into components.

Although the data set consists of ten-day composite images of the maximum NDVI, it was found that cloud contamination persists in the study area. Based on the cloud detection criteria implemented in this study, about 49% of the area on average was contaminated by clouds in the time period considered here. For such cloud contaminated images, it was found that working with preliminary classified homogeneous units, Terrain Mapping Units, is more realistic than working on a pixel basis. The level of consistency of the output results proved that the processing methodology developed in this work, may be of value for practical work.

In the absence of ground data and atmospheric composition measurements, during the times of the satellite overpass, the statistical approach for noise removal proved to be a reliable alternative for other atmospheric correction techniques.

It was found that images taken by NOAA-14 have higher pixel values than those of NOAA-11 in the different channels. In case of studying time series of images, care should be taken when the images are taken from different satellites because of the different calibration coefficients used for different sensors.

The smooth pattern of the Arctangent of the ratio between surface temperature and NDVI suggests that it is less sensitive to noise than the individual variables. The ratio also seems to be related to the resistance to evapotranspiration of the different land covers in the study area.

The surface temperature-NDVI ratio function seems to be highly correlated to the hydrological behavior of the different units in the catchment with respect to the evapotranspiration component of the hydrological cycle and consequently to the soil moisture content. So it is recommended that further research be done on this relation together with other parameters like rainfall to arrive at a regional estimation of evapotranspiration for the different units in the catchment.

Finally, work is under way to apply the techniques described here to raw NOAA data files from the Satellite Active Archive. This would allow construction of much larger time series of hydrological basins at low cost. However, geocorrection, radiometric and atmospheric corrections are then much more complicated.

Acknowledgements

The work was carried out in the framework of the Lake Naivasha Water Resources Assessment Project in co-operation with the Kenyan Water Resources and Environmental Division, financially supported by the Netherlands Government. The authors are greatly indebted to R. Becht for fieldwork guidance in Kenya, and the Kenyan Wildlife Services for providing logistical support.

References

Bastiaanssen, W.G.M., 1995. Regionalization of surface flux densities and moisture indicators in composite terrain, A remote sensing approach under clear skies in Mediterranean climates. PhD Thesis Wageningen University, The Netherlands, pp273.

Caselles, C.C., Sobrino, J.A. and Valor, E., 1994. On the Atmospheric Dependence of the Split Window Equation for Land Surface Temperature. International Journal of Remote Sensing, 15 (1), 105-122.

Eidenshink, J.C. and Faundeen, J.L. , 1994. The 1-km AVHRR Global Data Set: First Stages in Implementation. International Journal of Remote Sensing, 15, 3443-3462.

Goward, S.N., Markham, B., Dye, D.G., Dulaney, W. and Yang, J., 1991. Normalized Difference Vegetation Index Measurements from the Advanced Very High Resolution Radiometer. Remote Sensing of the Environment. 35, 257-277.

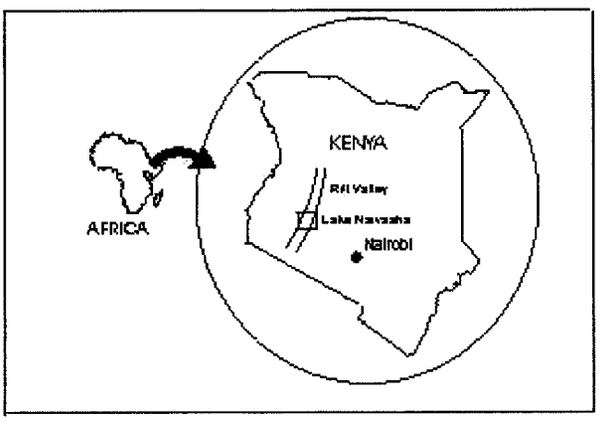

Fig. 1 Location map of the study area around Lake Naivasha (Kenya).

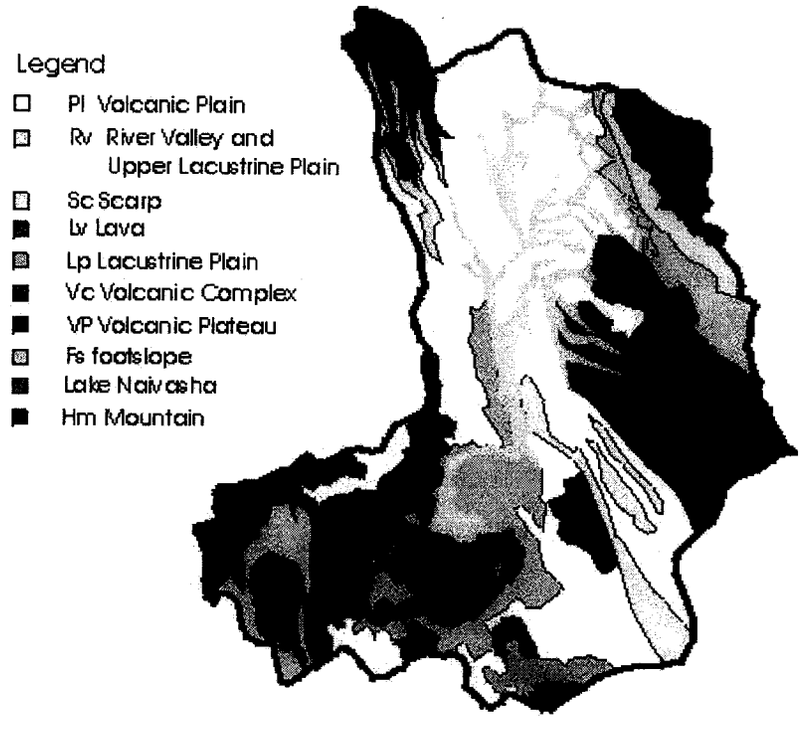

Fig. 2 Terrain Mapping Units after Hamududu (1998)

Fig. 3 NDVI image before application of the cloud detection and spatial filter.

Fig. 4 NDVI image after application of the cloud detection and spatial filter.

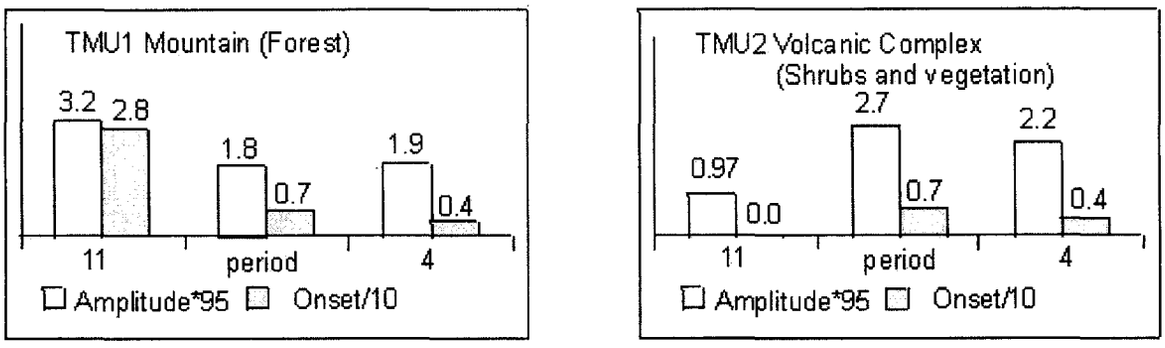

Fig. 5 Amplitude and Onset of the NDVI for two different TMU's in the catchment.

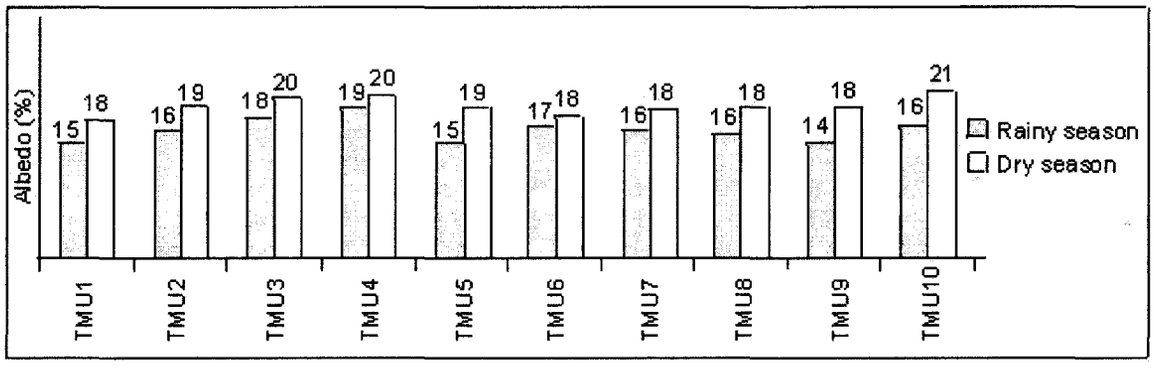

Fig. 6 Comparison between surface albedos of dry and wet seasons.

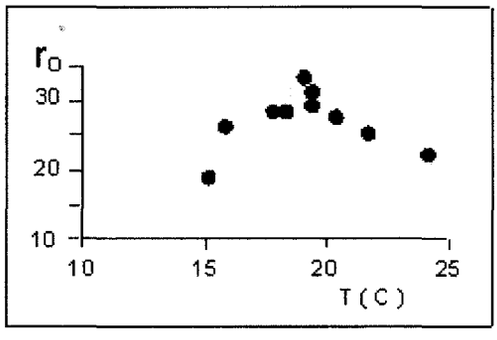

Fig. 7 Relation between Surface Temperature and Albedo (wet season)

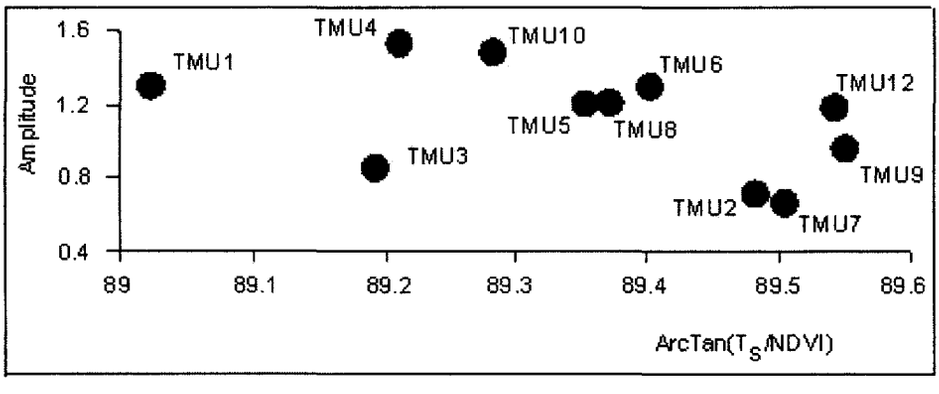

Fig. 8 Feature Space of the Amplitude and ArcTan(T_S/NDVI).

Gutman, G.G., 1991. Vegetation Indices from AVHRR: An Update and Future Prospects. Remote Sensing of Environment. 35, 121-136.

Hamududu, B.H., 1998. Erosion Assessment for Large Basins using Remote Sensing and GIS: a Case Study of Lake Naivasha Basin, Kenya. ITC MSc Thesis.

Lambin, E.F. and Ehrlich, D., 1996. The Surface Temperature-Vegetation Index Space for Land Cover and Land Cover Change Analysis. International Journal of Remote Sensing, 17(3), 463-487.

NOAA Technical Report NESDIS 49, 1990. Implementation of Reflectance Models in Operational AVHRR Radiation Budget Processing.

Saunders, R.W. and Kriebel, K.T., 1988. An Improved Method for Detecting Clear Sky and Cloudy Radiances from NOAA-AVHRR Data. International Journal of Remote Sensing, 9 (1), 123-150.

Van Dijk, A., Susan, L.C., Clarence, M.S. and Vayne, L.D., 1987. Smoothing Vegetation Index Profiles: An Alternative Method for Reducing Radiometric Disturbance in NOAA-AVHRR Data. Photogrametric Engineering and Remote Sensing, 53(8), 1059-1067.

Van de Griend, A.A. and Owe, M., 1993. On the Relationship between Thermal Emissivity and the Normalized Difference Vegetation Index for Natural Surfaces. International Journal of Remote Sensing, 14(6), 1119-1131.

Velleman, P. and Hoaglin, D.C., 1981. Applications, Basics and Computing of Exploratory Data Analysis. Duxbury Press, Boston, Mass.